Jens Ziegle*, Alfredo Illanes, Axel Boese and Michael Friebe

Frequency and average gray-level information for thermal ablation status in ultrasound B-Mode sequences

https://doi.org/10.1515/cdbme-2020-0023

Abstract: During thermal ablation in a target tissue the information about temperature is crucial for decision making of successful therapy. An observable temporal and spatial temperature propagation would give a visual feedback of irreversible cell damage of the target tissue. Potential temperature features in ultrasound (US) B-Mode image sequences during radiofrequency (RF) ablation in *ex-vivo* porcine liver were found and analysed. These features could help to detect the transition between reversible and irreversible damage of the ablated target tissue. Experimental RF ablations of *ex-vivo* porcine liver were imaged with US B-Mode imaging and image sequences were recorded. Temperature was simultaneously measured within the liver tissue around a bipolar RF needle electrode. In the B-Mode images, regions of interest (ROIs) around the centre of the measurement spots were analysed in post-processing using average gray-level (AVGL) compared against temperature. The pole of maximum energy level in the time-frequency domain of the AVGL changes was investigated in relation to the measured temperatures. Frequency shifts of the pole were observed which could be related to transitions between the states of tissue damage.

Keywords: B-mode imaging; liver ultrasound; medical imaging; radiofrequency ablation; thermal monitoring.

Introduction

Thermal therapies such as laser, microwave, radiofrequency (RF) ablation and high-intensity focused US (HIFU) are applied in clinical settings mainly for treatment of small carcinoma and metastases. These therapies are followed with image guidance for visualization of target tissue in combination with minimally invasive placement of therapy tools, e.g. one or more needle electrodes. The success of a thermal therapy relies on the thermal damage in the target tissue. Tissue exposed to a certain temperature level will undergo (i) reversible damage with ≤ 45 °C, (ii) irreversible cellular damage within 46–60 °C and (iii) instantaneous irreversible protein coagulation between 60–100 °C [1]. For such a therapy the assessment of temperature within the target tissue is necessary to guarantee a success of a complete treatment. Incomplete treatment increases the risk of recurrence of pathological tissue. In order to observe the progression of the thermal therapy a continuous temperature monitoring is needed.

Magnetic resonance imaging (MRI) has shown to be sufficient in temperature estimation and is preferred with the combination of HIFU system [2]. However, a combination with other ablation therapy systems such as RF ablation requires MRI compatible equipment. Additionally, high cost of such a clinical MR procedure, restricted range of motion for handling therapy tools inside the bore and system availability led to a motivation to search for alternative temperature monitoring systems. A more versatile alternative could be given by US imaging systems having the advantage of low investment costs and higher availability. In the past, several methods of temperature estimation using US imaging have been investigated. Two major approaches are: first, the change of speed of sound and second, variation in acoustic impedance and thus change in image contrast intensity caused by change in temperature within the tissue [3]. The SOS method has a limitation of temperature correlation to temperatures above 60 °C where a linear relation levels off [4]. Unfortunately, the range of temperature where instantaneous irreversible tissue damage occurs is above 60 °C [5]. In contrary, contrast intensity changes due to increased temperature can be obtained directly from the respective B-Mode images. During the ablation process the heated tissue has a loss of cell fluids which leads to a change in tissue density. Along the density change the acoustic impedance is meant to change which should affect the appearance of intensity, i.e. pixel gray-level in the US image. Gray-level changes during ablation could be used for correlation with temperature [6] or with ablation progression of the tissue. In past studies, an average gray-level (AVGL) [7]

***Corresponding author: Jens Ziegle**, Otto-von-Guericke-University, Medical Faculty, Magdeburg, Germany, E-mail: jens.ziegle@ovgu.de
Alfredo Illanes, Axel Boese and Michael Friebe, Otto-von-Guericke-University, Medical Faculty, Magdeburg, Germany

in a ROI within the target tissue resulted in a correlation to temperature with a coefficient of 0.88 for temperatures below 50 °C [6].

In this paper, we address the correlation of temperatures up to 75 °C to the relative AVGL change and their corresponding change in the frequency domain.

Material and methods

Image sequence acquisition

An experimental setup has been implemented where a slice of *ex-vivo* porcine liver was placed in a holding box on top of two layers of 15 mm thick US wave transmittable gel pads (Aquaflex, PARKER LABS., USA) to add depth and avoiding strong US wave reflections from the bottom. A LOGIQ E9 US imaging system was used in combination with a ML6-15 US transducer (GE, USA) operating at 12 MHz. The transducer was placed on top of the liver using a holding structure that additionally allows the attachment of a needle guide bracket (Verza, CIVCO, USA), as shown in Figure 1. The needle holder kept a bipolar RF needle in sight of the US image plane. A RF power of 25 W was applied using a bipolar RF ablation system (CelonPower, Olympus, Germany) together with a RF needle cooling system (Aquaflow III, Olympus, Germany). US image sequences were recorded using a frame grabber (USB3HD-CAP, StarTech, Canada) with 30 frames per second directly to a computer. The sequences included 90–120 s before the ablation start and at least 120 s of the cooling phase after the ablation stop. Simultaneously, temperatures inside the liver were acquired by an optical thermometry system (FOTEMP, Optocon, Germany) via four optical fibre sensors placed around the RF needle. The sampling rate of temperature acquisition was 1 Hz and the temperature data were interpolated to match the US image acquisition. The temperature and

Figure 1: Holding structure with porcine liver (A), holding box (B), Aquaflex gel pads (C), linear 9L probe (D), custom 3D printed transducer holder (E), Verza needle guide bracket (F) and bipolar RF needle (G).

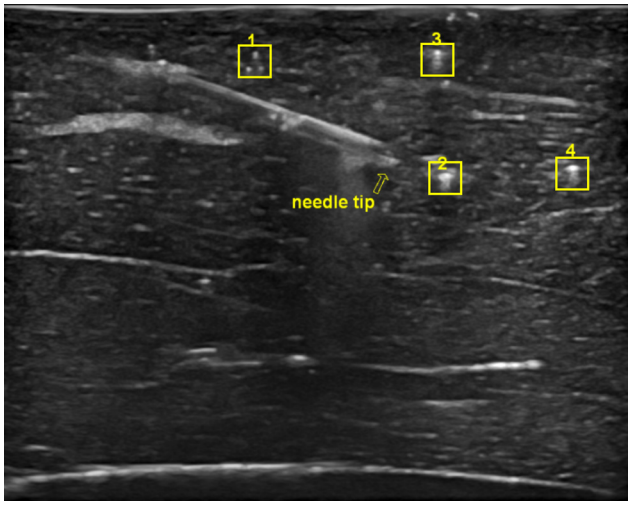

Figure 2: US image of *ex-vivo* liver piece with a placed RF needle inserted from left upper corner towards direction to the ROI number 2. Each selected ROI has a size of 1.8 × 1.8 mm and is centred on one of the four temperature sensor positions.

US data were recorded with the same computer and with timestamps. A total of 13 experiments were conducted, with four temperature measurement points each and with same US image settings including the same gain level of 68.

Image sequence processing

Average gray-level: For each experimental US sequence, ROIs were selected around the centre of the four temperature sensor positions as exemplary shown in Figure 2. ROI sizes of 31 × 31 pixel (1.8 × 1.8 mm) were chosen and an AVGL-ratio was calculated from each ROI per image in the B-Mode sequence as following:

$$\mathrm{AVGL_{ration}\,(n)} = \frac{\sum_{k=1}^{M}\sum_{l=1}^{N} p_{kl}\,(n)}{\sum_{k=1}^{M}\sum_{l=1}^{N} p_{kl}\,(n_1)}, \tag{1}$$

in which $p_{kl}(n)$ is the gray-level value of the pixel in the position kl at the image frame number n, n_1 is the first image frame, and M and N are the dimensions of the ROI. With Equation (1), the AVGL relative to the AVGL of the first image frame, i.e. first time instant, can be calculated over the US image sequence.

Average gray-level ratios at the instant when temperatures of 30–75 °C in steps of 5 °C were measured to examine the temperature relation. For each temperature level the AVGL-ratio distribution was observed to investigate the variance throughout the conducted experiments. Additionally, for each ROI the Pearson correlation coefficients between AVGL-ratio and measured temperature were computed. The variance and the Pearson correlation coefficient should lead to a statement whether a general correlation between an AVGL-ratio and temperature can be determined.

Frequency of average gray-level changes: The AVGL-ratio change was used to observe the progression of texture changes, i.e. the change of AVGL relative to the initial AVGL over time. By using this relative change, each ROI was normalized to its initial tissue texture

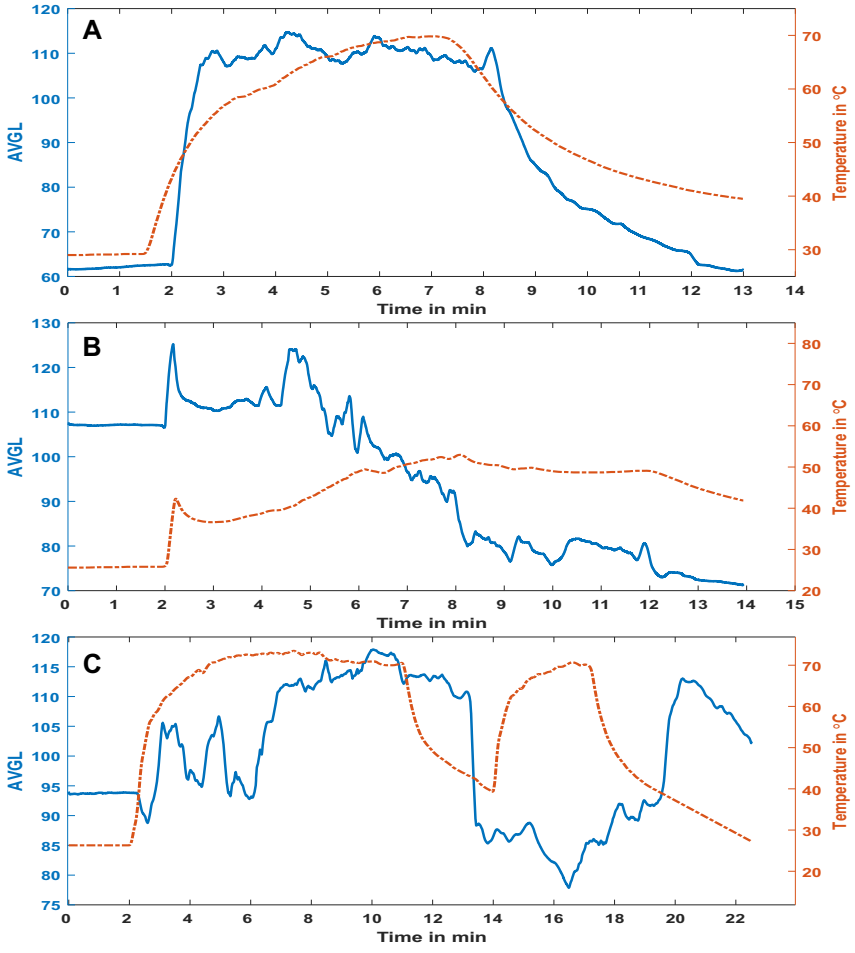

Figure 3: Examples (A, B, C) of AVGL change and the corresponding measured temperature change of ablation processes in three different experiments.

and thus should reduce the inter-variability in the conducted experiments. It had been reported that an exceeding over 60 °C in tissue leads to instantaneous irreversible cell damage called coagulation. It was assumed that a damage such as coagulation could increase the rate of change in the AVGL-ratio and thus could be a good indicator of transition in tissue ablation state. A rate of change in a signal can be described by the dynamics in the frequency spectrum over time. A time-variant autoregressive modelling is used to track the frequency changes in the spectrum. For that, a pole-based approach is used where at each time instant the

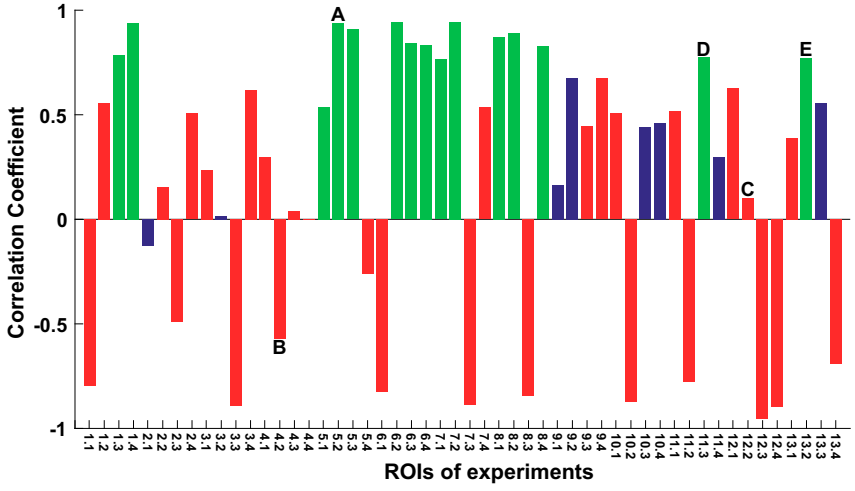

Figure 4: Pearson correlation coefficients of AVGL-ratio to temperature curves from 52 ROIs of 13 *ex-vivo* porcine liver experiments.

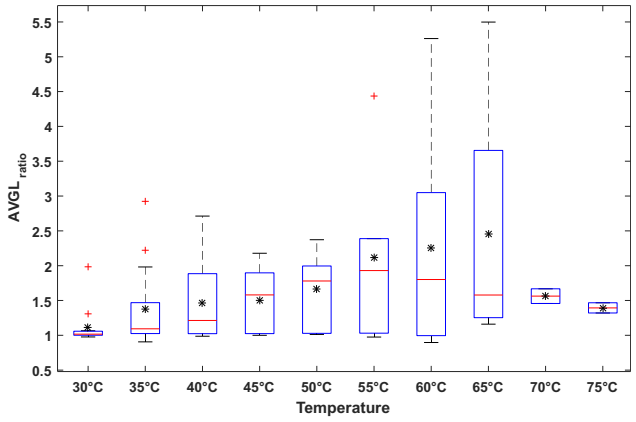

Figure 5: Distribution of AVGL-ratio from the 15 ROIs unaffected by texture shifts or shadow effects at discrete temperatures from 30 to 75 °C.

maximal energy pole is used for computation of the dominant frequency, as described in [8].

The instantaneous dominant frequency over time provides the information about prominent changes in the signal of AVGL-ratio, which could represent significant changes in tissue texture.

Results and discussion

Measurements and calculation from a total number of 52 ROIs in 13 experiments were performed. Figure 3 shows three example graphs of AVGL change of three different ROIs in three different ablation experiments with their corresponding measured temperature change, marked as A, B and C. In graph A the AVGL change follows the trend of the temperature change which resulted in a high correlation coefficient of 0.94, as indicated in Figure 4. The AVGL change in graph B follows the temperature trend in first 5 min and afterwards it continuously decreases. In this case, a shrinkage of liver tissue in proximity to the needle electrodes was observed, which pulled along the adjacent liver tissue. This movement shifted the tissue texture out of the observed ROI and caused the decrease in the AVGL. Consequently, the correlation between AVGL and temperature resulted in a low Pearson coefficient of −0.57 (see Figure 4). The negative sign indicates an inverse correlation, i.e. a high temperature corresponds to a low AVGL, or vice versa. In graph C the AVGL follows the trend of the temperature with some fluctuations between 3 and 6 min. As observed in the whole US image sequence, some bubble formation started from the needle electrodes and traversed towards this analysed ROI. The bubbles did not cross the ROI but shifted the analysed tissue texture out of the ROI. After disappearance of the bubbles the tissue texture moved back into the ROI. In the second increase of temperature at ~14 min an appearance of gas bubble formation led again to a shift of the observed tissue texture and resulted in a low Pearson coefficient of 0.1. The prior mentioned shift of texture out of the analysed ROI has a negative impact on the computing of the Pearson correlation coefficient between AVGL-ratio and temperature. Correlation coefficients for all ROIs are given in Figure 4.

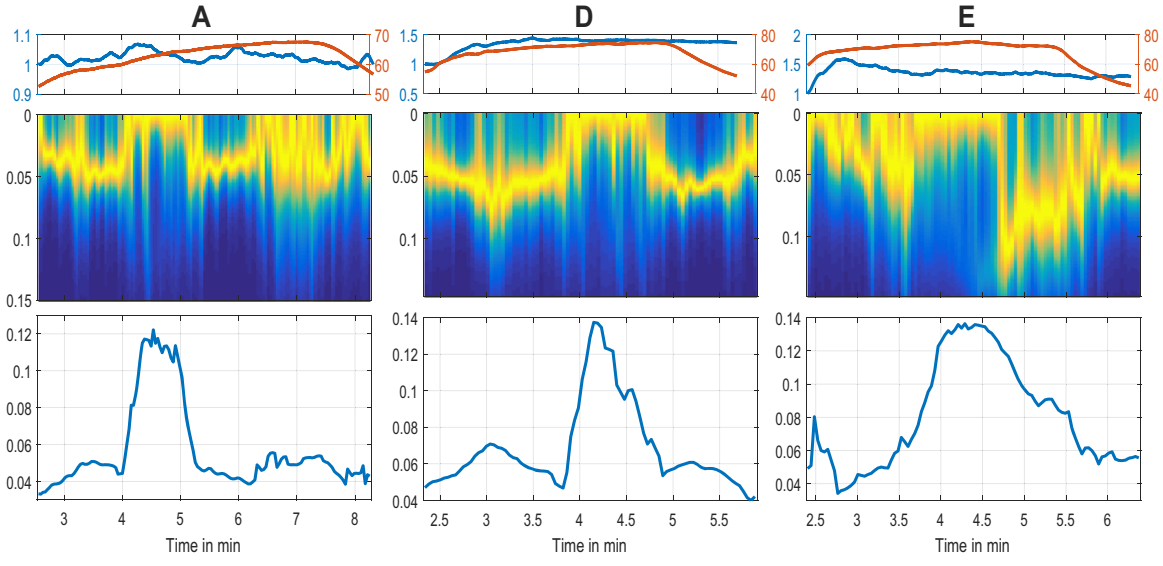

Figure 6: First row: AVGL-ratio (blue) with corresponding temperatures in °C (orange). Second row: spectrogram of lower frequencies in Hz. Third row: tracked pole of maximum energy. For three ROIs (A, D, E) unaffected by texture motion or shadow effect.

Minor or major shifts of texture, caused either by bubbles or tissue shrinkage affected 56% (29 of 52 ROIs) of the correlation results, as shown in red bars and resulted in an average coefficient of −0.12. 15% of ROIs (8 of 52) were affected by a shadow effect, where gas bubbles accumulated above the ROIs and blocked US waves which resulted in a shadow-like appearance in B-mode images. These cases are shown in blue bars and resulted in low correlations between AVGL-ratio and temperature, with an average coefficient of 0.31. In 29% of the ROIs (15 of 52) no shifts or shadow effect were observed, as marked as green bars. Without having the mentioned influences, an average correlation coefficient of 0.83 indicates that the AVGL-ratio could be used to observe the trend of temperature changes.

The distribution of AVGL-ratio at discrete temperatures from 30 to 75 °C is given in Figure 5 for the unaffected ROIs. With an increase of temperature the distribution spreads over a wider range of AVGL-ratio values. Thus, addressing an absolute AVGL-ratio to a temperature would be difficult. The more interesting information is included in its change of distribution over temperature increase, where the average and median is considered first. The average AVGL-ratios are marked as asterisks and show an increase up to a temperature of 65 °C. The median AVGL-ratio given in red horizontal lines start to drop earlier at 60 °C. Also in this temperature range of 60–65 °C the distribution of AVGL-ratios have a higher spread as indicated by the upper and lower quartiles and upper whiskers. The AVGL-ratio distribution suddenly drops at 70 °C and decreases further in 75 °C. This sudden drop could be a hint for an instant texture change such as the transition to coagulation, which is addressed to temperatures above 60 °C according to literature [6]. Figure 6 includes the frequency observations at temperatures higher than 50 °C of the AVGL-ratio, exemplary for three ROIs with high correlation (see A, D and E in Figure 4). In all three spectrograms, changes are present in the low frequency range between 0.01 and 0.15 Hz and shifts are visible after a temperature of 60 °C was exceeded. Also, the tracked pole of maximum energy of the spectrogram resulted in change towards higher frequency after temperature exceeded 60 °C. The rise of this pole towards higher frequency describes fast dynamics in the AVGL-ratio, i.e. the texture in the observed ROI changes faster during the time of applied high temperatures. This could be due to a transition of the tissue to a coagulated state, where tissue cells reach thermal equilibrium and clotting and solidification begins [6]. It has to be proven if the transition to coagulated tissue causes the shift in the tracked pole of maximum energy. In future experiments, it is planned to investigate the tissue ablation state after occurrence of the frequency shift in the pole. Therefore, the pathological findings of the tissue at this ablation state needs to be obtained.

Conclusion

The presented correlation of AVGL-ratio to temperature in experimental liver ablations was negatively affected by tissue movement induced by ablation effects. An absolute AVGL-ratio could not be related to a certain temperature but its trend of change could be correlated to the temperature trend. Dynamics of the change in AVGL-ratio in the frequency domain reacted with a frequency shift after exceeding a temperature of 60 °C. Coagulation mostly occurs at these temperatures and the frequency shifts could be related to it. The relation has to be investigated in further research.

Acknowledgment: Authors like to thank Olympus, Germany and GE Healthcare, USA for provision of the used medical equipment.
Research funding: The author state no funding involved.
Author contribution: All the authors have accepted responsibility for the entire content of this submitted manuscript and approved submission.
Competing interests: Authors state no conflict of interest.

References

1. McDermott S, Gervais DA. Radiofrequency ablation of liver tumors. Semin Intervent Radiol 2013;30:49–55.
2. Quesson B, de Zwart JA, Moonen CT. Magnetic resonance temperature imaging for guidance of thermotherapy. J Magn Reson Imag 2000;12:525–33.
3. Rivens I, Shaw A, Civale J, Morris H. Treatment monitoring and thermometry for therapeutic focused ultrasound. Int J Hyperther 2007;23:121–39.
4. Sun Z, Ying H. A multi-gate time-of-flight technique for estimation of temperature distribution in heated tissue: theory and computer simulation. Ultrasonics 1999;37:107–22.
5. Lewis MA, Staruch RM, Chopra R. Thermometry and ablation monitoring with ultrasound. Int J Hyperther 2015;31:163–81.
6. Teixeira CA, Alvarenga AV, Cortela G, Von Krüger MA, Pereira WC. Feasibility of non-invasive temperature estimation by the assessment of the average gray-level content of B-mode images. Ultrasonics 2014;54:1692.
7. Alvarenga AV, Wilkens V, Georg O, Costa-Félix RP. Non-invasive Estimation of Temperature during physiotherapeutic ultrasound application using the average gray-level content of B-Mode images: a metrological approach. Ultrasound Med Biol 2017;43:1938–52.
8. Illanes A, Boese A, Maldonado I, Pashazadeh A, Schaufler A, Navab N. Novel clinical device tracking and tissue characterization using proximally placed audio signal acquisition and processing. Sci Rep 2018;8.